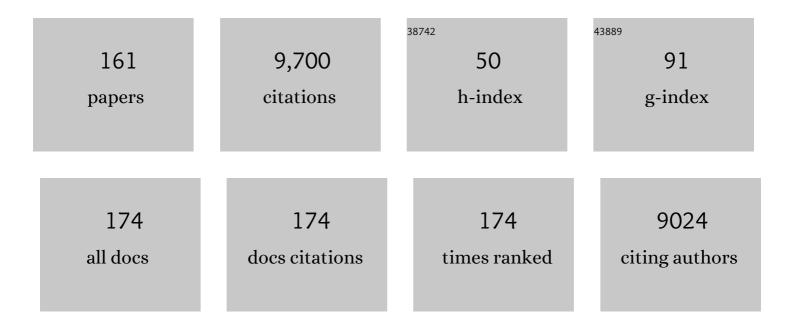
John A Mclean

List of Publications by Year in descending order

Source: https://exaly.com/author-pdf/1877638/publications.pdf Version: 2024-02-01



#	Article	IF	CITATIONS
1	Insights and prospects for ion mobility-mass spectrometry in clinical chemistry. Expert Review of Proteomics, 2022, , 1-15.	3.0	7
2	Improving confidence in lipidomic annotations by incorporating empirical ion mobility regression analysis and chemical class prediction. Bioinformatics, 2022, 38, 2872-2879.	4.1	5
3	Enantiomer Differentiation of Amino Acid Stereoisomers by Structural Mass Spectrometry Using Noncovalent Trinuclear Copper Complexes. Journal of the American Society for Mass Spectrometry, 2022, 33, 996-1002.	2.8	3
4	Collision Cross-Section Calibration Strategy for Lipid Measurements in SLIM-Based High-Resolution Ion Mobility. Journal of the American Society for Mass Spectrometry, 2022, 33, 1229-1237.	2.8	13
5	Preparation and characterization of discrete mass polyether-based polyurethane oligomers. Polymer, 2022, 254, 125069.	3.8	2
6	Genomic, transcriptomic, and metabolomic profiles of hiPSC-derived dopamine neurons from clinically discordant brothers with identical PRKN deletions. Npj Parkinson's Disease, 2022, 8, .	5.3	0
7	MYC regulates ribosome biogenesis and mitochondrial gene expression programs through its interaction with host cell factor–1. ELife, 2021, 10, .	6.0	45
8	Resolving Power and Collision Cross Section Measurement Accuracy of a Prototype High-Resolution Ion Mobility Platform Incorporating Structures for Lossless Ion Manipulation. Journal of the American Society for Mass Spectrometry, 2021, 32, 1126-1137.	2.8	43
9	Metabolomic Analysis Evidences That Uterine Epithelial Cells Enhance Blastocyst Development in a Microfluidic Device. Cells, 2021, 10, 1194.	4.1	3
10	Probing morphological, genetic and metabolomic changes of in vitro embryo development in a microfluidic device. Biotechnology Progress, 2021, 37, e3194.	2.6	5
11	Multidimensional Separations of Intact Phase II Steroid Metabolites Utilizing LC–Ion Mobility–HRMS. Analytical Chemistry, 2021, 93, 10990-10998.	6.5	18
12	Targeted and Untargeted Mass Spectrometry Reveals the Impact of High-Fat Diet on Peripheral Amino Acid Regulation in a Mouse Model of Alzheimer's Disease. Journal of Proteome Research, 2021, 20, 4405-4414.	3.7	6
13	Chlorpyrifos Disrupts Acetylcholine Metabolism Across Model Blood-Brain Barrier. Frontiers in Bioengineering and Biotechnology, 2021, 9, 622175.	4.1	7
14	High Confidence Shotgun Lipidomics Using Structurally Selective Ion Mobility-Mass Spectrometry. Methods in Molecular Biology, 2021, 2306, 11-37.	0.9	8
15	The acyl chains of phosphoinositide PIP3 alter the structure and function of nuclear receptor steroidogenic factor-1. Journal of Lipid Research, 2021, 62, 100081.	4.2	4
16	Accelerating strain phenotyping with desorption electrospray ionization-imaging mass spectrometry and untargeted analysis of intact microbial colonies. Proceedings of the National Academy of Sciences of the United States of America, 2021, 118, .	7.1	8
17	Mass spectrometry and ion mobility study of poly(ethylene glycol)â€based polyurethane oligomers. Rapid Communications in Mass Spectrometry, 2020, 34, e8662.	1.5	5
18	Defining a Molecular Signature for Uropathogenic versus Urocolonizing Escherichia coli: The Status of the Field and New Clinical Opportunities. Journal of Molecular Biology, 2020, 432, 786-804.	4.2	19

#	Article	IF	CITATIONS
19	An Integrative Gene Expression and Mathematical Flux Balance Analysis Identifies Targetable Redox Vulnerabilities in Melanoma Cells. Cancer Research, 2020, 80, 4565-4577.	0.9	6
20	Targeted Strategy to Analyze Antiepileptic Drugs in Human Serum by LC-MS/MS and LC-Ion Mobility-MS. Analytical Chemistry, 2020, 92, 14648-14656.	6.5	9
21	Chemical Class Prediction of Unknown Biomolecules Using Ion Mobility-Mass Spectrometry and Machine Learning: Supervised Inference of Feature Taxonomy from Ensemble Randomization. Analytical Chemistry, 2020, 92, 10759-10767.	6.5	13
22	Data highlighting phenotypic diversity of urine-associated Escherichia coli isolates. Data in Brief, 2020, 31, 105811.	1.0	9
23	Evaluating a targeted multiple reaction monitoring approach to global untargeted lipidomic analyses of human plasma. Rapid Communications in Mass Spectrometry, 2020, 34, e8911.	1.5	20
24	Accumulation of long-chain fatty acids in the tumor microenvironment drives dysfunction in in in intrapancreatic CD8+ T cells. Journal of Experimental Medicine, 2020, 217, .	8.5	142
25	Translational Roadmap for the Organs-on-a-Chip Industry toward Broad Adoption. Bioengineering, 2020, 7, 112.	3.5	52
26	Huntington's disease genotype suppresses global manganese-responsive processes in pre-manifest and manifest YAC128 mice. Metallomics, 2020, 12, 1118-1130.	2.4	17
27	Collision Cross Section Conformational Analyses of Bile Acids via Ion Mobility–Mass Spectrometry. Journal of the American Society for Mass Spectrometry, 2020, 31, 1625-1631.	2.8	13
28	Resolution of Isomeric Mixtures in Ion Mobility Using a Combined Demultiplexing and Peak Deconvolution Technique. Analytical Chemistry, 2020, 92, 9482-9492.	6.5	68
29	Algal Toxin Goniodomin A Binds Potassium Ion Selectively to Yield a Conformationally Altered Complex with Potential Biological Consequences. Journal of Natural Products, 2020, 83, 1069-1081.	3.0	9
30	Crowd-Sourced Chemistry: Considerations for Building a Standardized Database to Improve Omic Analyses. ACS Omega, 2020, 5, 980-985.	3.5	5
31	Fundamentals of Ion Mobility-Mass Spectrometry for the Analysis of Biomolecules. Methods in Molecular Biology, 2020, 2084, 1-31.	0.9	17
32	A Solution to Antifolate Resistance in Group B Streptococcus : Untargeted Metabolomics Identifies Human Milk Oligosaccharide-Induced Perturbations That Result in Potentiation of Trimethoprim. MBio, 2020, 11, .	4.1	25
33	Mass spectrometry of polyurethanes. Polymer, 2019, 181, 121624.	3.8	18
34	Spatiochemically Profiling Microbial Interactions with Membrane Scaffolded Desorption Electrospray Ionization-Ion Mobility-Imaging Mass Spectrometry and Unsupervised Segmentation. Analytical Chemistry, 2019, 91, 13703-13711.	6.5	23
35	Utilizing Untargeted Ion Mobility-Mass Spectrometry To Profile Changes in the Gut Metabolome Following Biliary Diversion Surgery. Analytical Chemistry, 2019, 91, 14417-14423.	6.5	9
36	Collision cross section compendium to annotate and predict multi-omic compound identities. Chemical Science, 2019, 10, 983-993.	7.4	196

#	Article	IF	CITATIONS
37	Recommendations for reporting ion mobility Mass Spectrometry measurements. Mass Spectrometry Reviews, 2019, 38, 291-320.	5.4	315
38	Alkali metal cation adduct effect on polybutylene adipate oligomers: Ion mobility-mass spectrometry. Polymer, 2019, 173, 58-65.	3.8	12
39	Evaluating Separation Selectivity and Collision Cross Section Measurement Reproducibility in Helium, Nitrogen, Argon, and Carbon Dioxide Drift Gases for Drift Tube Ion Mobility–Mass Spectrometry. Journal of the American Society for Mass Spectrometry, 2019, 30, 1059-1068.	2.8	32
40	lsomeric and Conformational Analysis of Small Drug and Drug-Like Molecules by Ion Mobility-Mass Spectrometry (IM-MS). Methods in Molecular Biology, 2019, 1939, 161-178.	0.9	1
41	New frontiers in lipidomics analyses using structurally selective ion mobility-mass spectrometry. TrAC - Trends in Analytical Chemistry, 2019, 116, 316-323.	11.4	37
42	Zinc intoxication induces ferroptosis in A549 human lung cells. Metallomics, 2019, 11, 982-993.	2.4	37
43	Predicting Ion Mobility Collision Cross-Sections Using a Deep Neural Network: DeepCCS. Analytical Chemistry, 2019, 91, 5191-5199.	6.5	121
44	lon mobility conformational lipid atlas for high confidence lipidomics. Nature Communications, 2019, 10, 985.	12.8	121
45	Organotypic Neurovascular Unit and Electrochemical Platform for Predictive Toxicology. ECS Meeting Abstracts, 2019, MA2019-02, 2423-2423.	0.0	0
46	Determining Double Bond Position in Lipids Using Online Ozonolysis Coupled to Liquid Chromatography and Ion Mobility-Mass Spectrometry. Analytical Chemistry, 2018, 90, 1915-1924.	6.5	69
47	Improving the discovery of secondary metabolite natural products using ion mobility–mass spectrometry. Current Opinion in Chemical Biology, 2018, 42, 160-166.	6.1	22
48	Automated flow injection method for the high precision determination of drift tube ion mobility collision cross sections. Analyst, The, 2018, 143, 1556-1559.	3.5	18
49	Conformational landscapes of ubiquitin, cytochrome c, and myoglobin: Uniform field ion mobility measurements in helium and nitrogen drift gas. International Journal of Mass Spectrometry, 2018, 427, 79-90.	1.5	71
50	Structural Characterization of Methylenedianiline Regioisomers by Ion Mobility-Mass Spectrometry and Tandem Mass Spectrometry. 4. 3-Ring and 4-Ring Isomers. Analytical Chemistry, 2018, 90, 14453-14461.	6.5	4
51	Untargeted Molecular Discovery in Primary Metabolism: Collision Cross Section as a Molecular Descriptor in Ion Mobility-Mass Spectrometry. Analytical Chemistry, 2018, 90, 14484-14492.	6.5	83
52	Chiral Separation Strategies in Mass Spectrometry: Integration of Chromatography, Electrophoresis, and Gas-Phase Mobility. , 2018, , 631-646.		3
53	Global untargeted serum metabolomic analyses nominate metabolic pathways responsive to loss of expression of the orphan metallo β-lactamase, MBLAC1. Molecular Omics, 2018, 14, 142-155.	2.8	11
54	An Integrated, High-Throughput Strategy for Multiomic Systems Level Analysis. Journal of Proteome Research, 2018, 17, 3396-3408.	3.7	32

#	Article	IF	CITATIONS
55	Chiral separation of diastereomers of the cyclic nonapeptides vasopressin and desmopressin by uniform field ion mobility mass spectrometry. Chemical Communications, 2018, 54, 9398-9401.	4.1	7
56	Integrated, High-Throughput, Multiomics Platform Enables Data-Driven Construction of Cellular Responses and Reveals Global Drug Mechanisms of Action. Journal of Proteome Research, 2017, 16, 1364-1375.	3.7	34
57	Investigation of the Complete Suite of the Leucine and Isoleucine Isomers: Toward Prediction of Ion Mobility Separation Capabilities. Analytical Chemistry, 2017, 89, 952-959.	6.5	74
58	Ion Mobility Collision Cross Section Compendium. Analytical Chemistry, 2017, 89, 1032-1044.	6.5	131
59	In Utero Exposure to Histological Chorioamnionitis Primes the Exometabolomic Profiles of Preterm CD4+ T Lymphocytes. Journal of Immunology, 2017, 199, 3074-3085.	0.8	12
60	Correlating Resolving Power, Resolution, and Collision Cross Section: Unifying Cross-Platform Assessment of Separation Efficiency in Ion Mobility Spectrometry. Analytical Chemistry, 2017, 89, 12176-12184.	6.5	126
61	An Interlaboratory Evaluation of Drift Tube Ion Mobility–Mass Spectrometry Collision Cross Section Measurements. Analytical Chemistry, 2017, 89, 9048-9055.	6.5	361
62	Structural Characterization of Methylenedianiline Regioisomers by Ion Mobility-Mass Spectrometry, Tandem Mass Spectrometry, and Computational Strategies. 3. MALDI Spectra of 2-Ring Isomers. Analytical Chemistry, 2017, 89, 9900-9910.	6.5	5
63	Comparative mass spectrometry-based metabolomics strategies for the investigation of microbial secondary metabolites. Natural Product Reports, 2017, 34, 6-24.	10.3	122
64	Metabolic consequences of inflammatory disruption of the blood-brain barrier in an organ-on-chip model of the human neurovascular unit. Journal of Neuroinflammation, 2016, 13, 306.	7.2	129
65	Targeting the untargeted in molecular phenomics with structurally-selective ion mobility-mass spectrometry. Current Opinion in Biotechnology, 2016, 39, 192-197.	6.6	25
66	Determination of ion mobility collision cross sections for unresolved isomeric mixtures using tandem mass spectrometry and chemometric deconvolution. Analytica Chimica Acta, 2016, 939, 64-72.	5.4	19
67	Untargeted Metabolomics Strategies—Challenges and Emerging Directions. Journal of the American Society for Mass Spectrometry, 2016, 27, 1897-1905.	2.8	789
68	Lipid profiling of polarized human monocyte-derived macrophages. Prostaglandins and Other Lipid Mediators, 2016, 127, 1-8.	1.9	31
69	Advanced Multidimensional Separations in Mass Spectrometry: Navigating the Big Data Deluge. Annual Review of Analytical Chemistry, 2016, 9, 387-409.	5.4	70
70	Evaluation of Collision Cross Section Calibrants for Structural Analysis of Lipids by Traveling Wave Ion Mobility-Mass Spectrometry. Analytical Chemistry, 2016, 88, 7329-7336.	6.5	148
71	Organs-on-Chips as Bridges for Predictive Toxicology. Applied in Vitro Toxicology, 2016, 2, 97-102.	1.1	23
72	Novel behavior of the chromatographic separation of linear and cyclic polymers. Analytical and Bioanalytical Chemistry, 2016, 408, 677-681.	3.7	7

#	Article	IF	CITATIONS
73	Aqueous Epoxide Ring-Opening Polymerization (AEROP): Green Synthesis of Polyglycidol with Ultralow Branching. Macromolecules, 2016, 49, 2022-2027.	4.8	22
74	Systems-Wide High-Dimensional Data Acquisition and Informatics Using Structural Mass Spectrometry Strategies. Clinical Chemistry, 2016, 62, 77-83.	3.2	25
75	A uniform field ion mobility study of melittin and implications of lowâ€field mobility for resolving fine crossâ€sectional detail in peptide and protein experiments. Proteomics, 2015, 15, 2862-2871.	2.2	20
76	Real-Time Cellular Exometabolome Analysis with a Microfluidic-Mass Spectrometry Platform. PLoS ONE, 2015, 10, e0117685.	2.5	24
77	Structural Characterization of Methylenedianiline Regioisomers by Ion Mobility-Mass Spectrometry, Tandem Mass Spectrometry, and Computational Strategies. 2. Electrospray Spectra of 3-Ring and 4-Ring Isomers. Analytical Chemistry, 2015, 87, 6288-6296.	6.5	20
78	Broadscale resolving power performance of a high precision uniform field ion mobility-mass spectrometer. Analyst, The, 2015, 140, 6824-6833.	3.5	45
79	Ion Mobility-Mass Spectrometry: Time-Dispersive Instrumentation. Analytical Chemistry, 2015, 87, 1422-1436.	6.5	322
80	Wavelet-Based Peak Detection and a New Charge Inference Procedure for MS/MS Implemented in ProteoWizard's msConvert. Journal of Proteome Research, 2015, 14, 1299-1307.	3.7	38
81	Non-derivatized glycan analysis by reverse phase liquid chromatography and ion mobility-mass spectrometry. Analyst, The, 2015, 140, 3335-3338.	3.5	34
82	Mapping Microbial Response Metabolomes for Induced Natural Product Discovery. ACS Chemical Biology, 2015, 10, 1998-2006.	3.4	79
83	MALDI-TOF/TOF CID study of poly(1,4-dihydroxybenzene terephthalate) fragmentation reactions. Polymer, 2015, 64, 100-111.	3.8	2
84	Profiling and Imaging Ion Mobility-Mass Spectrometry Analysis of Cholesterol and 7-Dehydrocholesterol in Cells Via Sputtered Silver MALDI. Journal of the American Society for Mass Spectrometry, 2015, 26, 924-933.	2.8	43
85	Structuring Microbial Metabolic Responses to Multiplexed Stimuli via Self-Organizing Metabolomics Maps. Chemistry and Biology, 2015, 22, 661-670.	6.0	40
86	Untargeted metabolic profiling identifies interactions between Huntington's disease and neuronal manganese status. Metallomics, 2015, 7, 363-370.	2.4	36
87	An Iron-Regulated Autolysin Remodels the Cell Wall To Facilitate Heme Acquisition in Staphylococcus lugdunensis. Infection and Immunity, 2015, 83, 3578-3589.	2.2	23
88	lon mobility-mass spectrometry strategies for untargeted systems, synthetic, and chemical biology. Current Opinion in Biotechnology, 2015, 31, 117-121.	6.6	39
89	Metabolic consequences of interleukin-6 challenge in developing neurons and astroglia. Journal of Neuroinflammation, 2014, 11, 183.	7.2	28
90	Systems-level view of cocaine addiction: The interconnection of the immune and nervous systems. Experimental Biology and Medicine, 2014, 239, 1433-1442.	2.4	16

#	Article	IF	CITATIONS
91	Distance Geometry Protocol to Generate Conformations of Natural Products to Structurally Interpret Ion Mobility-Mass Spectrometry Collision Cross Sections. Journal of Physical Chemistry B, 2014, 118, 13812-13820.	2.6	9
92	Unusual Kinetic Isotope Effects of Deuterium Reinforced Polyunsaturated Fatty Acids in Tocopherol-Mediated Free Radical Chain Oxidations. Journal of the American Chemical Society, 2014, 136, 838-841.	13.7	42
93	Conformational Ordering of Biomolecules in the Gas Phase: Nitrogen Collision Cross Sections Measured on a Prototype High Resolution Drift Tube Ion Mobility-Mass Spectrometer. Analytical Chemistry, 2014, 86, 2107-2116.	6.5	349
94	Structural mass spectrometry of tissue extracts to distinguish cancerous and non-cancerous breast diseases. Molecular BioSystems, 2014, 10, 2827-2837.	2.9	10
95	Structural Characterization of Methylenedianiline Regioisomers by Ion Mobility-Mass Spectrometry, Tandem Mass Spectrometry, and Computational Strategies: I. Electrospray Spectra of 2-Ring Isomers. Analytical Chemistry, 2014, 86, 4362-4370.	6.5	24
96	Phenotypic Mapping of Metabolic Profiles Using Self-Organizing Maps of High-Dimensional Mass Spectrometry Data. Analytical Chemistry, 2014, 86, 6563-6571.	6.5	37
97	Phosphorylation of Serine 106 in Asef2 Regulates Cell Migration and Adhesion Turnover. Journal of Proteome Research, 2014, 13, 3303-3313.	3.7	4
98	Bond-Specific Dissociation Following Excitation Energy Transfer for Distance Constraint Determination in the Gas Phase. Journal of the American Chemical Society, 2014, 136, 13363-13370.	13.7	40
99	The influence of drift gas composition on the separation mechanism in traveling wave ion mobility spectrometry: insight from electrodynamic simulations. International Journal for Ion Mobility Spectrometry, 2013, 16, 85-94.	1.4	24
100	Engineering Challenges for Instrumenting and Controlling Integrated Organ-on-Chip Systems. IEEE Transactions on Biomedical Engineering, 2013, 60, 682-690.	4.2	155
101	Antimicrobial drug resistance affects broad changes in metabolomic phenotype in addition to secondary metabolism. Proceedings of the National Academy of Sciences of the United States of America, 2013, 110, 2336-2341.	7.1	80
102	Neurovascular unit on a chip: implications for translational applications. Stem Cell Research and Therapy, 2013, 4, S18.	5.5	56
103	Structural Separations by Ion Mobility-MS for Glycomics and Glycoproteomics. Methods in Molecular Biology, 2013, 951, 171-194.	0.9	29
104	Glia co-culture with neurons in microfluidic platforms promotes the formation and stabilization of synaptic contacts. Lab on A Chip, 2013, 13, 3008.	6.0	99
105	Biomolecular Signatures of Diabetic Wound Healing by Structural Mass Spectrometry. Analytical Chemistry, 2013, 85, 3651-3659.	6.5	18
106	Semitransparent Nanostructured Films for Imaging Mass Spectrometry and Optical Microscopy. Analytical Chemistry, 2012, 84, 10665-10670.	6.5	9
107	Combined Elemental and Biomolecular Mass Spectrometry Imaging for Probing the Inventory of Tissue at a Micrometer Scale. Analytical Chemistry, 2012, 84, 3170-3178.	6.5	56
108	A Dual-Column Solid Phase Extraction Strategy for Online Collection and Preparation of Continuously Flowing Effluent Streams for Mass Spectrometry. Analytical Chemistry, 2012, 84, 8467-8474.	6.5	16

#	Article	IF	CITATIONS
109	Ag44(SR)304â^': a silver–thiolate superatom complex. Nanoscale, 2012, 4, 4269.	5.6	154
110	Structural Mass Spectrometry: Rapid Methods for Separation and Analysis of Peptide Natural Products. Journal of Natural Products, 2012, 75, 48-53.	3.0	32
111	Biomimetic monolayer-protected gold nanoparticles for immunorecognition. Nanoscale, 2012, 4, 3843.	5.6	22
112	Structural resolution of carbohydrate positional and structural isomers based on gas-phase ion mobility-mass spectrometry. Physical Chemistry Chemical Physics, 2011, 13, 2196-2205.	2.8	142
113	Lipid analysis and lipidomics by structurally selective ion mobility-mass spectrometry. Biochimica Et Biophysica Acta - Molecular and Cell Biology of Lipids, 2011, 1811, 935-945.	2.4	192
114	Multiplexed analysis of peptide functionality using lanthanide-based structural shift reagents. International Journal of Mass Spectrometry, 2011, 307, 28-32.	1.5	11
115	Nanoscale Phase Segregation of Mixed Thiolates on Gold Nanoparticles. Angewandte Chemie - International Edition, 2011, 50, 10554-10559.	13.8	74
116	Dual Source Ion Mobility-Mass Spectrometer for Direct Comparison of Electrospray Ionization and MALDI Collision Cross Section Measurements. Analytical Chemistry, 2010, 82, 3247-3254.	6.5	26
117	Characterization of thiolate-protected gold nanoparticles by mass spectrometry. Analyst, The, 2010, 135, 868.	3.5	90
118	Factors That Influence Helical Preferences for Singly Charged Gas-Phase Peptide Ions: The Effects of Multiple Potential Charge-Carrying Sites. Journal of Physical Chemistry B, 2010, 114, 809-816.	2.6	31
119	Structural Characterization of Phospholipids and Peptides Directly from Tissue Sections by MALDI Traveling-Wave Ion Mobility-Mass Spectrometry. Analytical Chemistry, 2010, 82, 1881-1889.	6.5	88
120	Identification of Phosphorylation Sites within the Signaling Adaptor APPL1 by Mass Spectrometry. Journal of Proteome Research, 2010, 9, 1541-1548.	3.7	19
121	Surface Fragmentation of Complexes from Thiolate Protected Gold Nanoparticles by Ion Mobility-Mass Spectrometry. Analytical Chemistry, 2010, 82, 3061-3066.	6.5	53
122	A Structural Mass Spectrometry Strategy for the Relative Quantitation of Ligands on Mixed Monolayer-Protected Gold Nanoparticles. Analytical Chemistry, 2010, 82, 9268-9274.	6.5	37
123	Structural mass spectrometry analysis of lipid changes in a Drosophila epilepsy model brain. Molecular BioSystems, 2010, 6, 958.	2.9	23
124	Peptide quantitation using primary amine selective metal chelation labels for mass spectrometry. Chemical Communications, 2010, 46, 5479.	4.1	12
125	Structurally Selective Imaging Mass Spectrometry by Imaging Ion Mobility-Mass Spectrometry. Methods in Molecular Biology, 2010, 656, 363-383.	0.9	7
126	The Conformational Landscape of Biomolecules in Ion Mobility–Mass Spectrometry. , 2010, , 327-343.		0

John A Mclean

#	Article	IF	CITATIONS
127	Chiral and structural analysis of biomolecules using mass spectrometry and ion mobilityâ€mass spectrometry. Chirality, 2009, 21, E253-64.	2.6	57
128	Characterizing ion mobility-mass spectrometry conformation space for the analysis of complex biological samples. Analytical and Bioanalytical Chemistry, 2009, 394, 235-244.	3.7	184
129	The mass-mobility correlation redux: The conformational landscape of anhydrous biomolecules. Journal of the American Society for Mass Spectrometry, 2009, 20, 1775-1781.	2.8	84
130	Adenylation Enzyme Characterization Using \hat{I}^3 -18O4-ATP Pyrophosphate Exchange. Chemistry and Biology, 2009, 16, 473-478.	6.0	52
131	Simultaneous glycoproteomics on the basis of structure using ion mobility-mass spectrometry. Molecular BioSystems, 2009, 5, 1298.	2.9	47
132	Labeling strategies in mass spectrometry-based protein quantitation. Analyst, The, 2009, 134, 1525.	3.5	20
133	Biomolecular structural separations by ion mobility–mass spectrometry. Analytical and Bioanalytical Chemistry, 2008, 391, 905-909.	3.7	147
134	Characterization of Branching in Aramid Polymers Studied by MALDIâ^'Ion Mobility/Mass Spectrometry. Macromolecules, 2008, 41, 8299-8301.	4.8	37
135	Enhanced carbohydrate structural selectivity in ion mobility-mass spectrometry analyses by boronic acid derivatization. Chemical Communications, 2008, , 5505.	4.1	47
136	Profiling and imaging of tissues by imaging ion mobilityâ€mass spectrometry. Journal of Mass Spectrometry, 2007, 42, 1099-1105.	1.6	202
137	Spatially dynamic laser patterning using advanced optics for imaging matrix assisted laser desorption/ionization (MALDI) mass spectrometry. International Journal of Mass Spectrometry, 2007, 262, 256-262.	1.5	10
138	A collision cross-section database of singly-charged peptide ions. Journal of the American Society for Mass Spectrometry, 2007, 18, 1232-1238.	2.8	77
139	The influence and utility of varying field strength for the separation of tryptic peptides by ion mobility-mass spectrometry. Journal of the American Society for Mass Spectrometry, 2005, 16, 158-165.	2.8	35
140	Ion mobility–mass spectrometry: a new paradigm for proteomics. International Journal of Mass Spectrometry, 2005, 240, 301-315.	1.5	282
141	Size-Selected (2â^'10 nm) Gold Nanoparticles for Matrix Assisted Laser Desorption Ionization of Peptides. Journal of the American Chemical Society, 2005, 127, 5304-5305.	13.7	370
142	Peak capacity of ion mobility mass spectrometry: the utility of varying drift gas polarizability for the separation of tryptic peptides. Journal of Mass Spectrometry, 2004, 39, 361-367.	1.6	83
143	Determination of Depleted Uranium in Urine via Isotope Ratio Measurements Using Large-Bore Direct Injection High Efficiency Nebulizer—Inductively Coupled Plasma Mass Spectrometry. Applied Spectroscopy, 2004, 58, 1044-1050.	2.2	23
144	A High Repetition Rate (1 kHz) Microcrystal Laser for High Throughput Atmospheric Pressure MALDI-Quadrupole-Time-of-Flight Mass Spectrometry. Analytical Chemistry, 2003, 75, 648-654.	6.5	38

#	Article	IF	CITATIONS
145	Sub-Femtomole Peptide Detection in Ion Mobility-Time-of-Flight Mass Spectrometry Measurements. Journal of Proteome Research, 2003, 2, 427-430.	3.7	33
146	Determination of Memory-Prone Elements Using Direct Injection High Efficiency Nebulizer Inductively Coupled Plasma Mass Spectrometry. Applied Spectroscopy, 2002, 56, 1006-1012.	2.2	26
147	Axial inductively coupled plasma time-of-flight mass spectrometry using direct liquid sample introduction. Journal of Analytical Atomic Spectrometry, 2002, 17, 669-675.	3.0	28
148	Determination of 236U/238U isotope ratio in contaminated environmental samples using different ICP-MS instruments. Journal of Analytical Atomic Spectrometry, 2002, 17, 958-964.	3.0	76
149	Oligonucleotide analysis with MALDI–ion-mobility–TOFMS. Analytical and Bioanalytical Chemistry, 2002, 373, 612-617.	3.7	70
150	A direct injection high efficiency nebulizer interface for microbore high-performance liquid chromatography-inductively coupled plasma mass spectrometry. Journal of Analytical Atomic Spectrometry, 2001, 16, 852-857.	3.0	42
151	Spatial aerosol characteristics of a direct injection high efficiency nebulizer via optical patternation. Spectrochimica Acta, Part B: Atomic Spectroscopy, 2001, 56, 1113-1126.	2.9	24
152	Ultratrace and isotopic analysis of long-lived radionuclides by double-focusing sector field inductively coupled plasma mass spectrometry using direct liquid sample introduction. International Journal of Mass Spectrometry, 2001, 208, 193-204.	1.5	46
153	Determination of Chromium in Human Lung Fibroblast Cells Using a Large Bore—Direct Injection High-Efficiency Nebulizer with Inductively Coupled Plasma Mass Spectrometry. Applied Spectroscopy, 2000, 54, 659-663.	2.2	34
154	A Large Bore-Direct Injection High Efficiency Nebulizer for Inductively Coupled Plasma Spectrometry. Analytical Chemistry, 2000, 72, 1885-1893.	6.5	74
155	Optical Patternation:  A Technique for Three-Dimensional Aerosol Diagnostics. Analytical Chemistry, 2000, 72, 4796-4804.	6.5	23
156	Internalization of Carcinogenic Lead Chromate Particles by Cultured Normal Human Lung Epithelial Cells: Formation of Intracellular Lead-Inclusion Bodies and Induction of Apoptosis. Toxicology and Applied Pharmacology, 1999, 161, 240-248.	2.8	105
157	Ultratrace and Isotope Analysis of Long-Lived Radionuclides by Inductively Coupled Plasma Quadrupole Mass Spectrometry Using a Direct Injection High Efficiency Nebulizer. Analytical Chemistry, 1999, 71, 3077-3084.	6.5	92
158	Fundamental Properties of Aerosols Produced in Helium by a Direct Injection Nebulizer. Applied Spectroscopy, 1999, 53, 1331-1340.	2.2	23
159	Nebulizer diagnostics: fundamental parameters, challenges, and techniques on the horizon. Journal of Analytical Atomic Spectrometry, 1998, 13, 829-842.	3.0	77
160	A Direct Injection High-Efficiency Nebulizer for Inductively Coupled Plasma Mass Spectrometry. Analytical Chemistry, 1998, 70, 1012-1020.	6.5	176
161	Sensitive Quantitation of Chromium-DNA Adducts by Inductively Coupled Plasma Mass Spectrometry with a Direct Injection High-Efficiency Nebulizer. Toxicological Sciences, 1998, 46, 260-265.	3.1	38